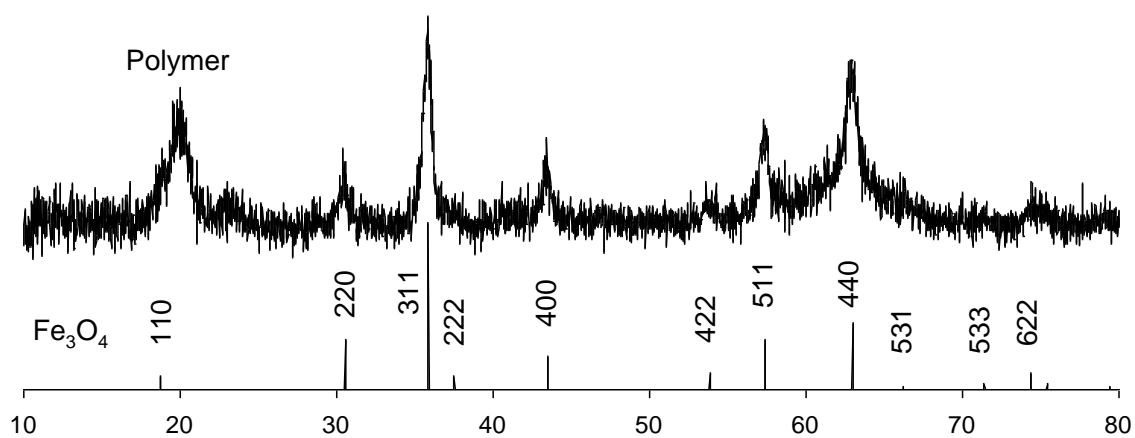
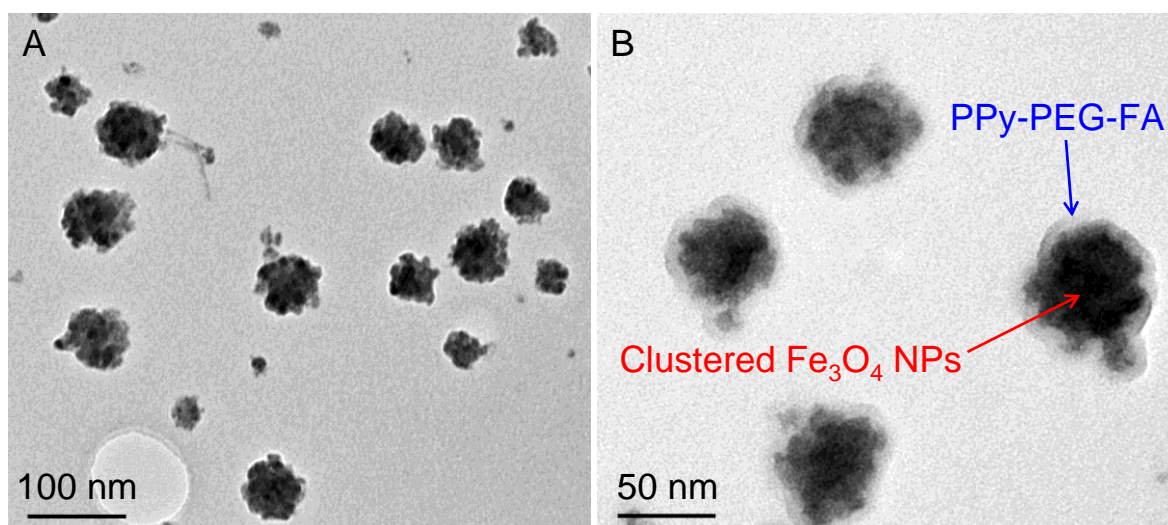


## Supplementary Material



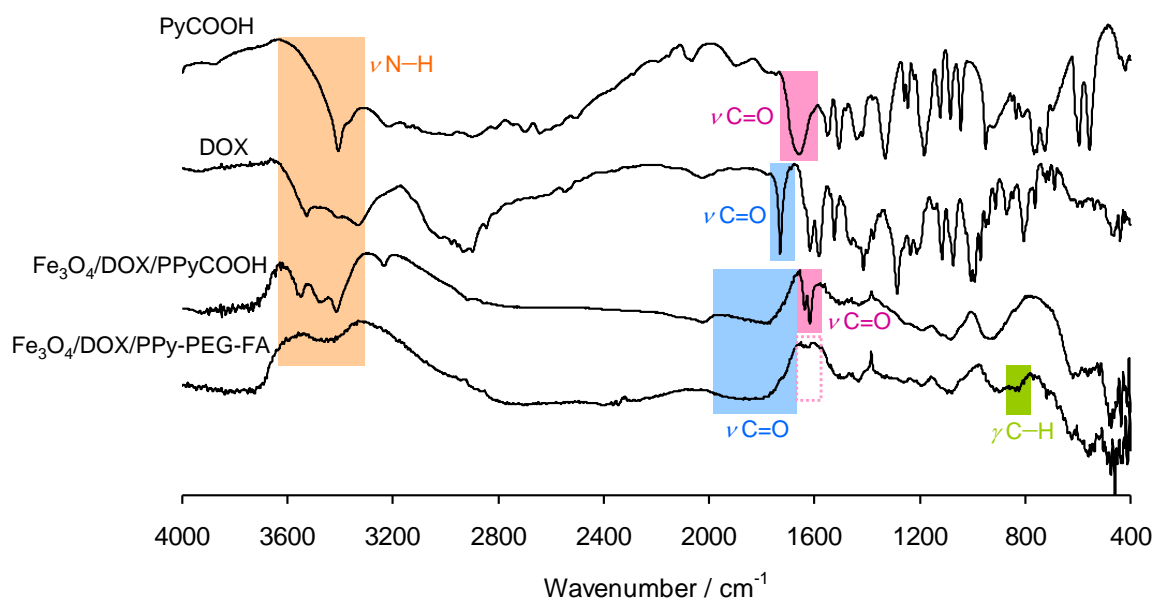


Figure S3. FTIR spectra of PyCOOH, DOX, Fe<sub>3</sub>O<sub>4</sub>/DOX/PPyCOOH NPs, and Fe<sub>3</sub>O<sub>4</sub>/DOX/PPy-PEG-FA NPs: the bands corresponding to the amine ( $\nu$  N-H) of pyrrole ring, DOX and FA (orange box); the bands attributed to the carboxylic acid ( $\nu$  C=O) bound to pyrrole ring (pink box); the bands attributed to the carboxylic acid ( $\nu$  C=O) of DOX (blue box); the band attributed to the aromatic hydrocarbon of FA (green box); The dotted pink box indicates that the bands attributed to the carboxylic acid of PPyCOOH disappear by amidation between Fe<sub>3</sub>O<sub>4</sub>/DOX/PPyCOOH NPs and FA-PEG-NH<sub>2</sub>.

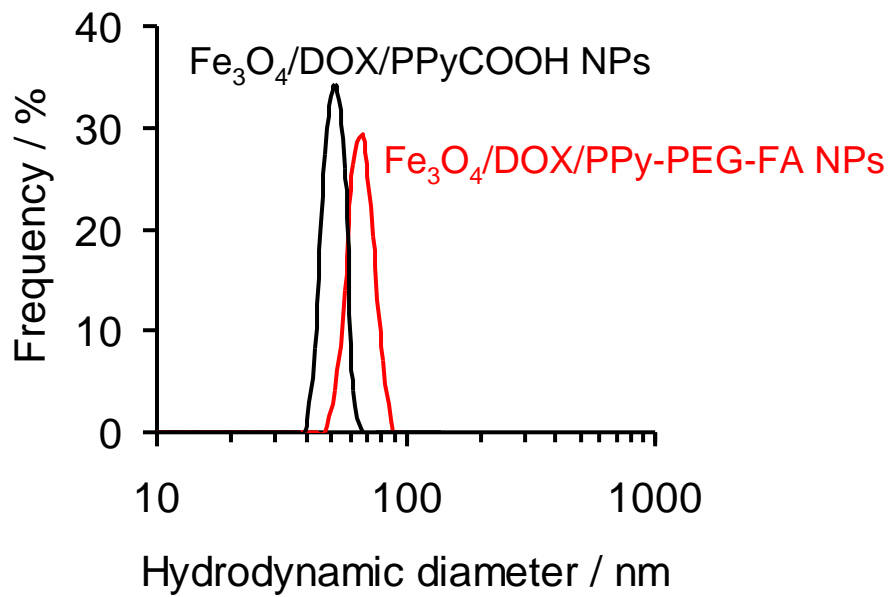


Figure S4. Hydrodynamic diameter of Fe<sub>3</sub>O<sub>4</sub>/DOX/PPyCOOH NPs and Fe<sub>3</sub>O<sub>4</sub>/DOX/PPy-PEG-FA NPs in water.

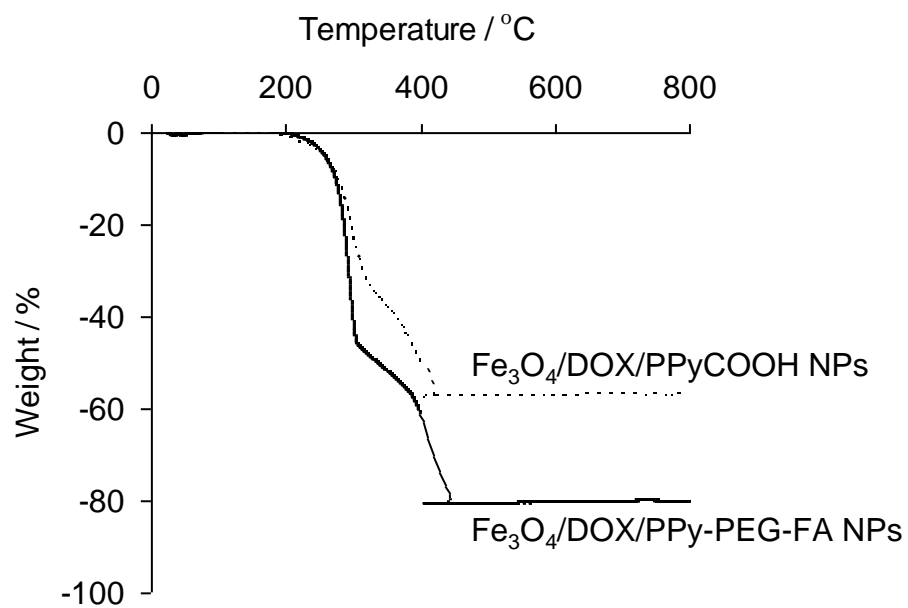


Figure S5. TG curves of Fe<sub>3</sub>O<sub>4</sub>/DOX/PPyCOOH NPs (dotted line) and Fe<sub>3</sub>O<sub>4</sub>/DOX/PPy-PEG-FA NPs (solid line).

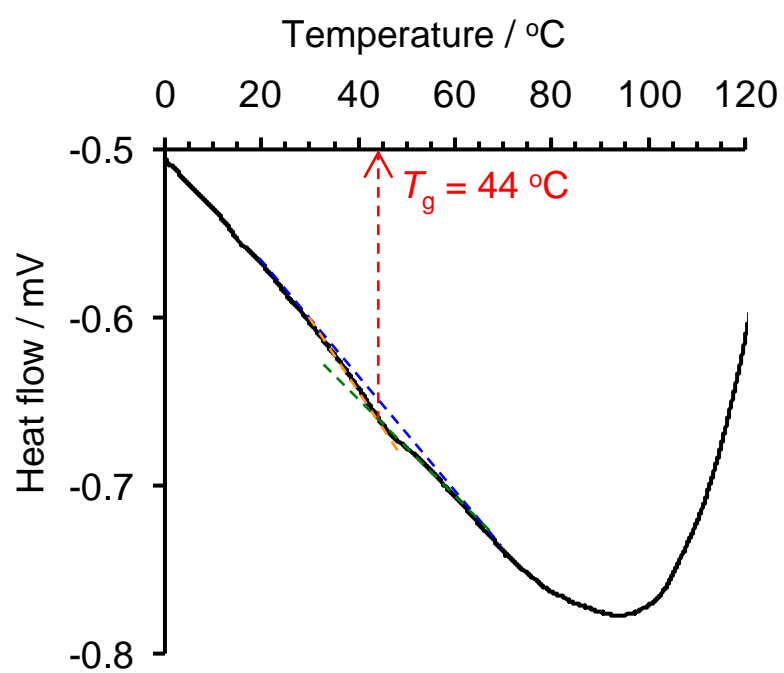


Figure S6. DSC curves of  $\text{Fe}_3\text{O}_4/\text{DOX}/\text{PPyCOOH}$  NPs and  $\text{Fe}_3\text{O}_4/\text{DOX}/\text{PPy-PEG-FA}$  NPs.

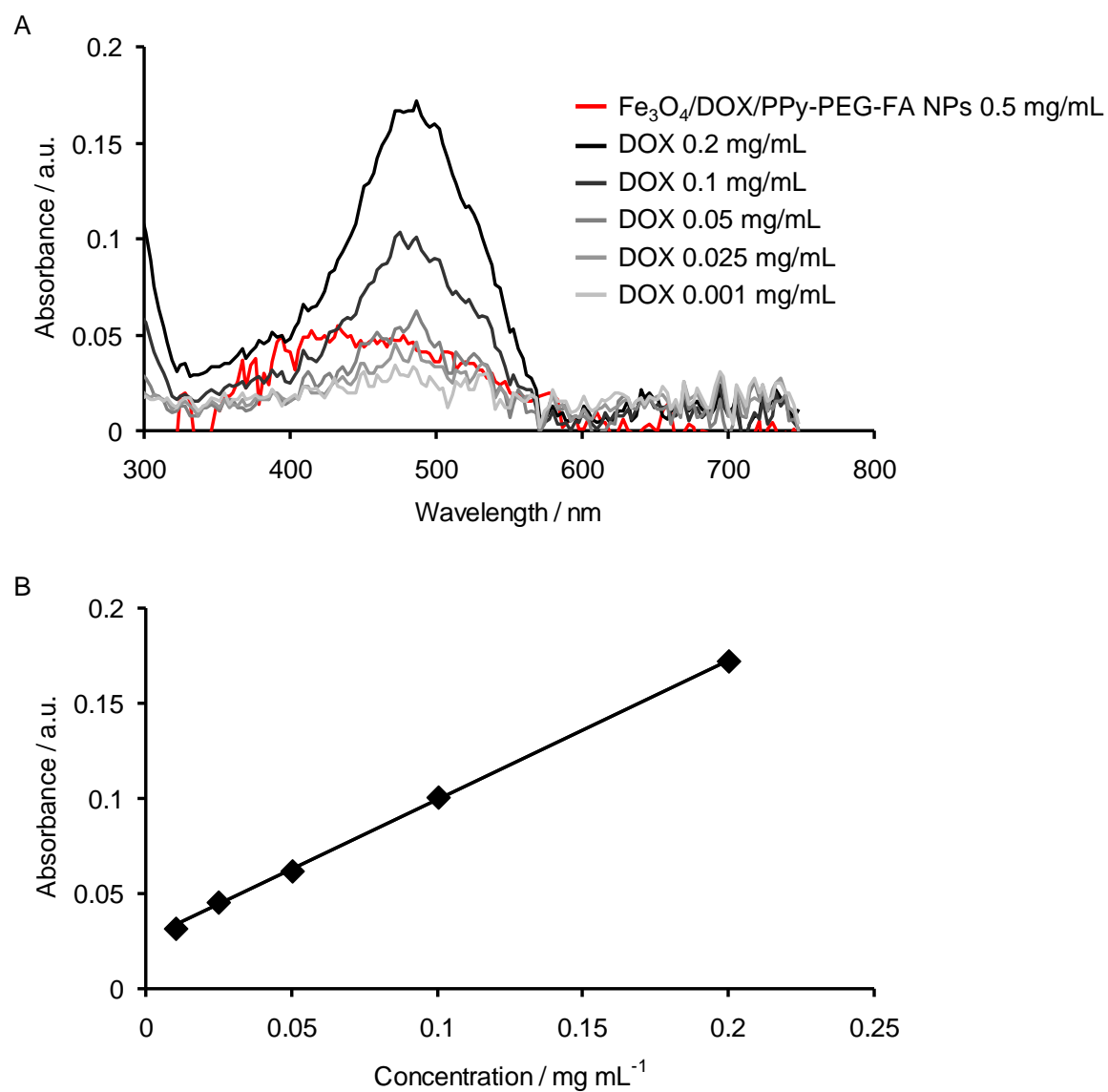


Figure S7. (A) Absorption spectra of Fe<sub>3</sub>O<sub>4</sub>/DOX/PPy-PEG-FA NPs and DOX in water. (B) Calibration curve prepared using the data of Figure S7A.

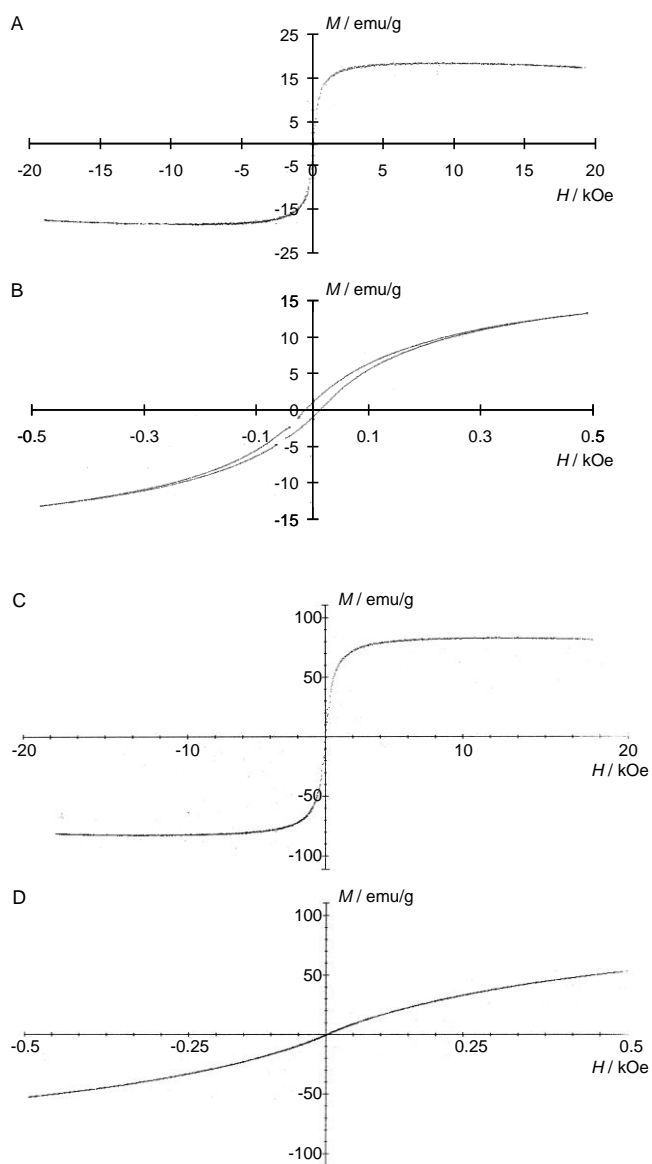


Figure S8. (A) Magnetization curves of Fe<sub>3</sub>O<sub>4</sub>/DOX/PPy-PEG-FA NPs. (B) Magnified view of the origin in Figure S8A. (C) Magnetization curves of Fe<sub>3</sub>O<sub>4</sub> NPs synthesized by mixing FeCl<sub>3</sub> with hydrazine. (D) Magnified view of the origin in Figure S8C.

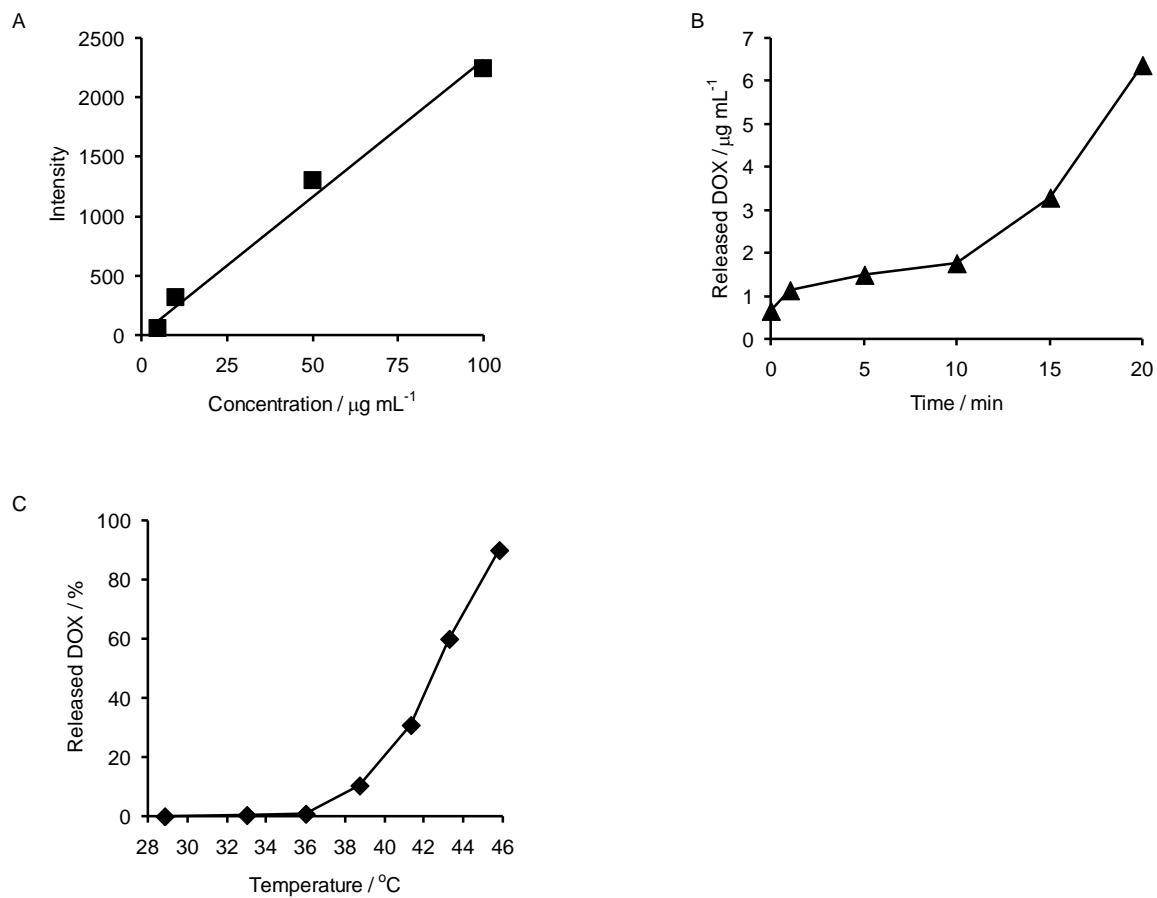


Figure S9. (A) Fluorescence intensity as a function of the concentration of DOX (calibration curve). (B) The amount of DOX released from  $\text{Fe}_3\text{O}_4/\text{DOX}/\text{PPy-PEG-FA}$  NPs with time of ACMF exposure. (C) Proportion of DOX released from  $\text{Fe}_3\text{O}_4/\text{DOX}/\text{PPy-PEG-FA}$  NPs with respect to temperature.

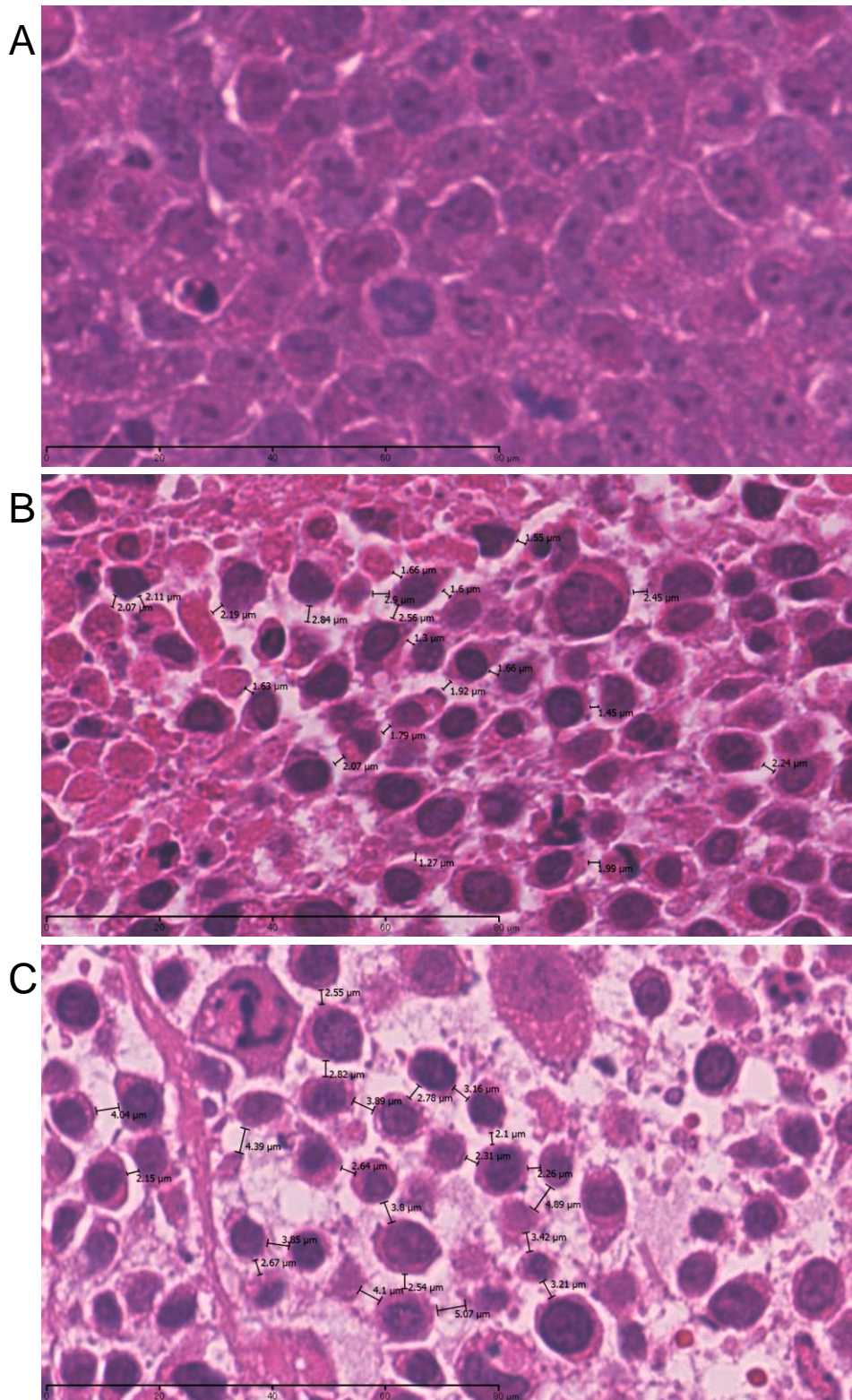


Figure S10. Magnified histological findings of the tumor of the mice in Figure 4: (A) non-treated mice, (B) mice treated with MHT and (C) mice treated with the combination of MHT and chemotherapy. The spaces between the cancer cells of the tumors treated by only MHT and the

combination of MHT and chemotherapy are estimated to be 0.5–3  $\mu\text{m}$  and 2–5  $\mu\text{m}$ , respectively, whereas the cancer cells are packed with no space between them in non-treated tumor.

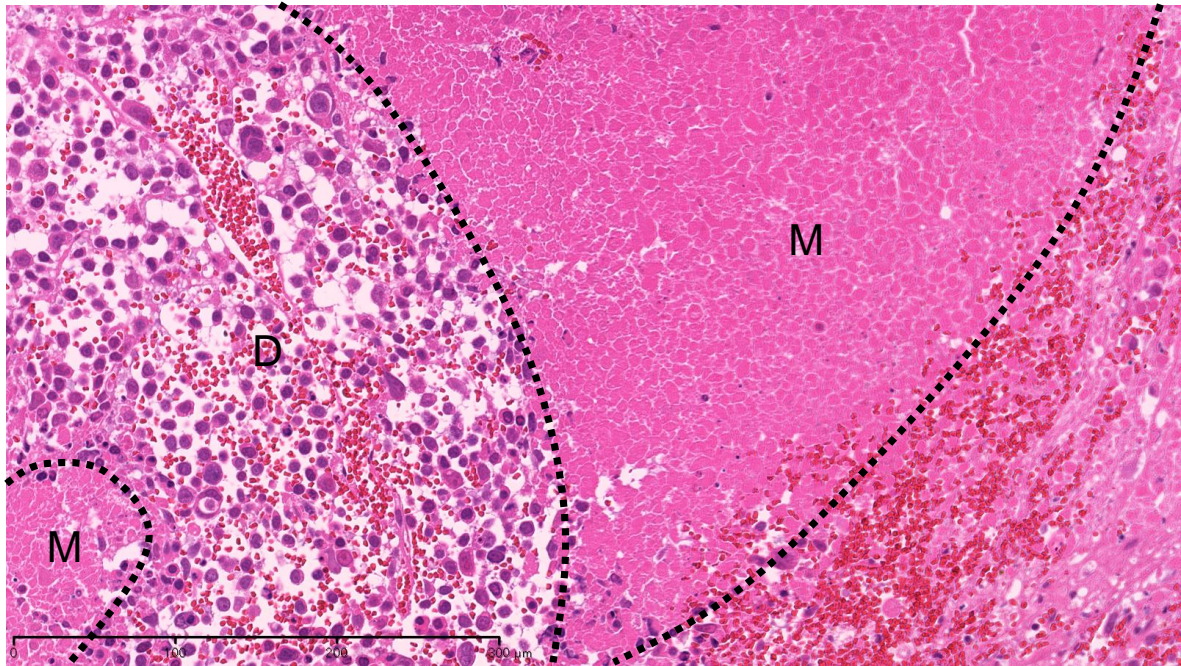


Figure S11. Magnified histological findings of the tumor of the mice treated with a combination of MHT and chemotherapy 24 h after the treatment in Figure 4: normal muscle tissue (M); destroyed tumor tissue (D).

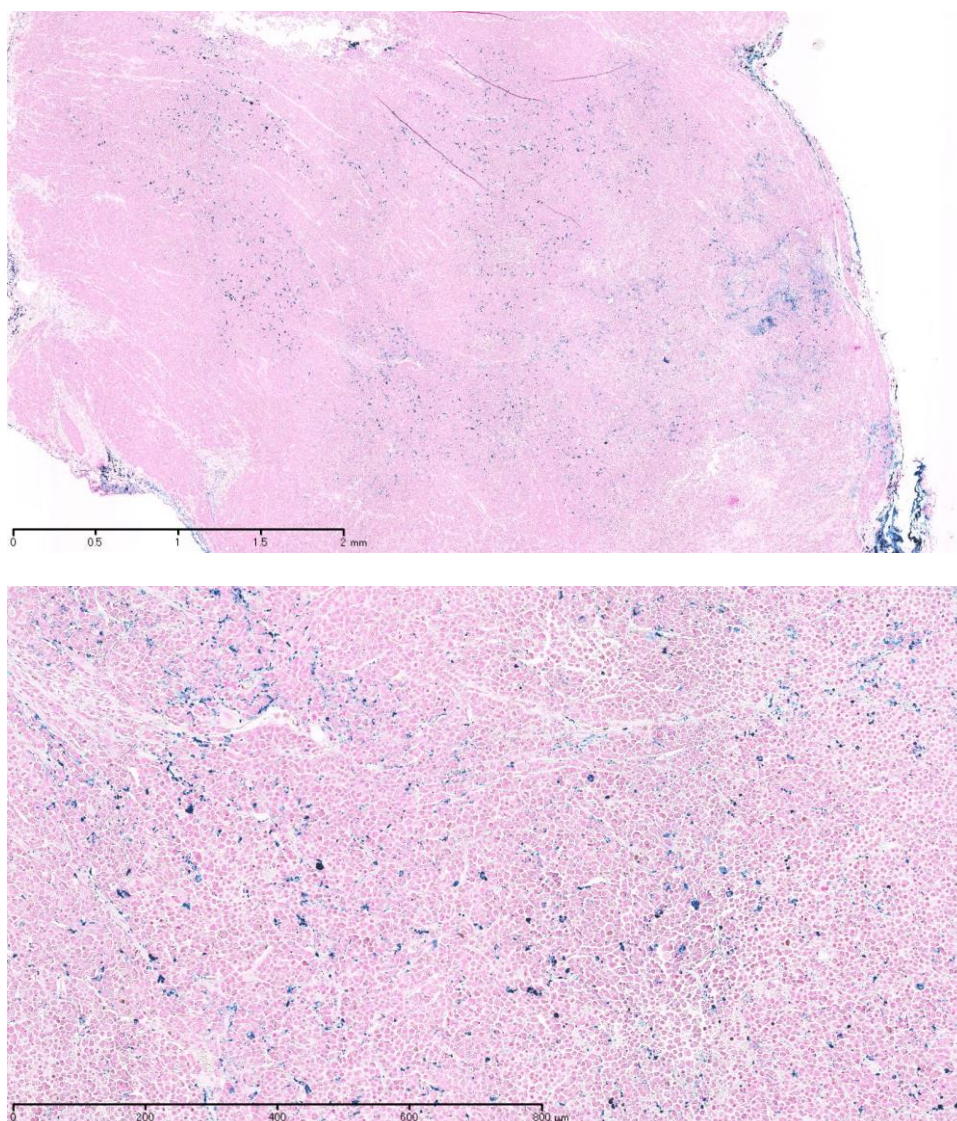


Figure S12. Prussian blue nuclear fast red staining of the tumor of the mice treated with a combination of MHT and chemotherapy 24 h after the treatment: iron is stained blue.